Spatio-temporal variability in stable isotopes of Brahmaputra river system

Madhusmita Nanda and Archana M. Nair*

Earth System Science and Engineering Division, Department of Civil Engineering, Indian Institute of Technology Guwahati, Guwahati–781039, India

*Corresponding author.

E-mail address: nair.archana@iitg.ac.in

ABSTRACT

The Brahmaputra river system is one of Asia's largest and most dynamic transboundary rivers. Yet, significant investigations on the isotopic signature of its water are limited and not documented. This study aims to address the limitations in datasets and enhance the knowledge of the river's complex hydrological processes and its climatic influence using the stable isotope technique. Over 1-2 years, a comprehensive dataset of isotopes was gathered from multiple locations within the basin to study the continuous changes in precipitation, groundwater, and surface water. Seasonal observations were also conducted along different parts of the lower Brahmaputra river system, from its entry point in Indian territory to its lower reaches in the Assam valley. The isotopic composition reflects contributions from various sources such as glacial melt, snowfall, rainfall, and groundwater that flow into the river water. Seasonal isotopic variations in precipitation show depleted signatures during the post-monsoon due to intense rainout, resulting in enrichment in the remaining water vapour. Enriched values of precipitation during the pre-monsoon indicate significant evaporation. Spatial variation in river water points to isotopic depletion in upstream regions due to snowmelt and glacial contributions, while downstream reaches display isotopic enrichment from heavy precipitation

inputs and tributary influence. The result of distinct isotopic signatures in different reaches of the river is due to variations in basin characteristics. It helps to understand water sources, evaporation-precipitation dynamics, and regional hydrological processes. These findings would contribute to developing a better knowledge of the hydrological behaviour of the Brahmaputra River and help in taking appropriate measures for crucial management of water resources and predicting climate change impacts on river systems.

Keywords: Brahmaputra river; Stable isotope; Precipitation; Subsurface flow; Surface runoff; Glacier melt.

1. Introduction

Major river systems (e.g., Indus, Ganga, and Brahmaputra) originating from the Hindu Kush Himalaya are the primary components of the hydrological cycle in South Asia. The region is considered as the largest reservoir of ice after polar regions and acts as the source of moisture recycling and carrier of large amounts of water, sediment and nutrients to the ocean (Scott et al., 2019). The region has the largest biodiversity, with the vast human population residing in a fragile ecosystem (Bookhagen and Burbank, 2010; Burkhart et al., 2017). Climate change and land use land cover alteration due to various anthropogenic activities are adversely affecting the region (Piao et al., 2010).

Hence, investigation is required for sustainable water resource management and understanding of the river system (Vörösmarty et al., 2010). Generally, various techniques are used for hydrological process investigation such as isotope tracers (Banda et al., 2024; Jeelani et al., 2017; Klaus and McDonnell, 2013; Nan et al., 2021; Rai et al., 2017; Ren et al., 2016; Zhou et al., 2015), hydrological modelling (Lindström et al., 2010; Rautela et al., 2023; Singh et al., 2008; Swain et al., 2018), and remote sensing (Aggarwal et al., 2020; Gaur et al., 2022; Taia et al., 2023). However, the isotopic tracer technique is more effective in understanding the complexity of the hydrological system. Generally, in hydrological studies using the isotopic tracer technique, stable isotopes of oxygen and hydrogen are considered (Diamond, 2022; Gat, 2010; Vitvar et al., 2005). The variation in isotopic ratios for various hydrologic components are result of phase changes and mixing. Globally, the correlation that exists between $\delta^{18}O$ and δD in precipitation is represented as the Global Meteoric Water Line (GMWL) (Craig, 1961; Dansgaard, 1964; Kumar et al., 2010; Rozanski et al., 1993). The variation found in the isotopic signature of precipitation is due to the effect of altitude as well as the fractionation of snow and melt components, especially in higher altitudes.

Thus, variation in the isotopic signature at different stages within the hydrological system is regulated by processes like evaporation, condensation, precipitation, and runoff (Mook, 2001) (Fig. 1). The evaporation from larger water bodies and oceans carries lighter isotopes easily than heavier isotopes which result in the enrichment of lighter isotopes in water vapour left behind isotopically heavier water (Gat and Gonfiantini, 1981; Gat et al., 2000). Similarly, heavier isotopes preferentially condense into raindrops during condensation, resulting in the initial precipitation with isotopic enrichment. As the cloud moves towards the landmass from the oceanside, the isotopic signature of the precipitation gradually gets depleted (Kumar et al., 2010). Therefore, the moisture that transports to the higher altitudes are fractionated further, resulting in a more depleted isotopic signature for the precipitation in the form of snow (Gat and Gonfiantini, 1981; Gat, 1996; Gat et al., 2000). Subsequently, the meltwater from snow and glaciers carries a depleted isotopic signature due to the melting of glaciers and ice sheets. Gradually, this meltwater contributes to the surface runoff, integrating various watersheds and different components, creating a mixed isotopic signature for river water (Gat, 2010; Mook, 2001). Further, this water infiltrates into the groundwater system, adding to the subsurface flow and resulting in isotopic fractionation due to evaporation, recharge and mixing with the old water. Groundwater generally preserves the isotopic signature of the precipitation that recharged it unless mixed with other sources of water (Deshpande et al., 2003; Krishan et al., 2023; Mazor, 1990).

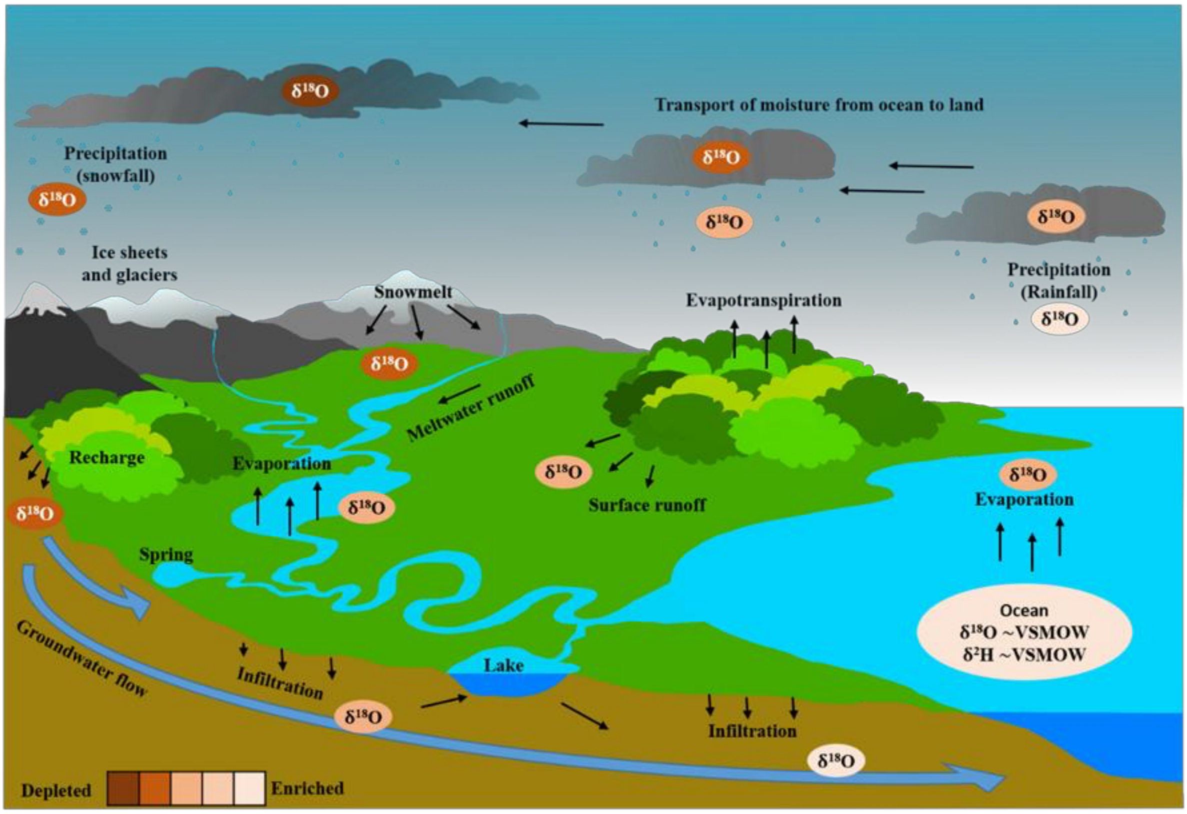

Fig. 1. Schematic illustration of the variations in isotopic signatures ($\delta^{18}O$ and $\delta^{2}H$) throughout different stages of the hydrological cycle. The diagram highlights how ocean evaporation enriches water vapour with lighter isotopes, while precipitation favours heavier isotopes, leading to a depletion of lighter isotopes in residual moisture. It also illustrates the impact of altitude and the fractionation processes involved in snow and melt runoff, surface runoff, and subsurface flow.

The Brahmaputra river system is considered one of the largest river systems in South Asia, stretching over multiple climate zones and vast geographic regions starting from Tibet. The river is known to be originating from the glaciers (such as Chemayungdung glacier, Kubi glacier, and Angsi glacier) near Manasarowar in the Kailash range, travelling through the plains of Assam and reaching the Bay of Bengal through the Bengal plains (Pranavananda, 1939;

Goswami, 1985; Singh et al., 2004). As a result, this river system exhibits a complex hydrology with spatial and temporal variability in isotopic signature. Brahmaputra river system caters to a population of 83 million, spread over four countries, with the highest percentage residing in Bangladesh (41%) and in the state of Assam, India (34%) (Singh et al., 2004). The adverse effects of climate change on glaciers affect the total water budget, resulting in large variability in hydrological processes (Gao, 2019). For example, large-scale variability of river discharge due to the shrinking of glaciers affects the quality and quantity of river water, impacting the livelihood of the vast population residing in such regions.

Numerous researchers have studied hydrological processes in river systems using stable isotope techniques (Gao et al., 2021; Pandey et al., 2023; Penna et al., 2014; Rai et al., 2021; Terzer et al., 2013; Wu et al., 2019). Considering the importance of such studies, the International Atomic Energy Agency (IAEA) has established a Global Network of Isotopes in Precipitation (GNIP) and a Global Network of Isotopes in Rivers (GNIR) (Rozanski et al., 2013; Vitvar et al., 2012). However, there is a scarcity of data related to isotope variability for the Brahmaputra river basin. Few studies using the stable isotope technique on the Brahmaputra river are primarily focused on specific sections of the river or small catchments. Kumar et al. (2010) reported isotopic variability in Guwahati from July 2003 to October 2004. Various studies at Jorhat were also reported for spatio-temporal variability in the moisture sources (Ganguly et al., 2023; Jeelani et al., 2018). Laskar et al. (2015) established the Local Meteoric Water Line at Hailakandi, Assam, Northeast India, from June 2009 to July 2011. Boral and Sen (2020) used the data available from different literature (Bershaw et al., 2012; Hren et al., 2009; Ren et al., 2016) to study the Yarlung Tsangpo part of the Brahmaputra river system. Additionally, the study by Hren et al. (2009) was conducted on the upper Brahmaputra region (Tsangpo and upper part of Siang river) almost two decades ago (Aug 1998, May 1999, Apr 2005, and Feb 2006) and lacks temporal variability of $\delta^{18}O$ and δD signature in the river water.

The isotopic variability in groundwater, river water, snow and glaciers has not been extensively investigated. Therefore, there is a need to study the spatio-temporal complexity in stable isotope variability for the entire Brahmaputra river system.

Unfortunately, the scarcity of systematic isotopic investigation in the Brahmaputra river system limits a comprehensive understanding of hydrological processes. The spatiotemporal patterns of $\delta^{18}O$ and δD in precipitation are missing for the entire reach of the river system. The present study aims to cover the data gap in the whole reach of the Brahmaputra system and improve the understanding of hydrological processes dominating the flow characteristics. Therefore, comprehensive isotope data has been collected systematically from the high mountainous regions, such as the Khangeri glacier and the Mago basin, to the river's lower reach at Golpara from July 2022- July 2024. To investigate the temporal variability in the isotopic signature of the river water, groundwater and precipitation, a systematic continuous monitoring station is established at Guwahati. River water samples from the main channel of the Brahmaputra, groundwater samples, and precipitation samples were collected continuously from October 2022 to July 2024. Another station has been established in Naharlagun, Itanagar, for spatial variability in precipitation. This study seeks to construct reference data for future climate change scenarios, insight into the hydrological processes, and reconstruction of past climate scenarios. The outcome of this study provides spatiotemporal variability in precipitation and its moisture source in the Brahmaputra system, insight into the seasonal variability in snow and glaciers in this region, and groundwater and river water variability across space and time.

2. Material and methods

2.1. Study area

This study focuses on the main headwater region of the Brahmaputra basin, located in the north-eastern part of India. Out of the total catchment area of the Brahmaputra river, India covers 33.6 %, which is shared by Arunachal Pradesh, Assam, Nagaland, Meghalaya, Sikkim, and West Bengal, whereas the large area percentage covered by Arunachal Pradesh and Assam around 41.88% and 36.33%, respectively (Singh et al., 2004). The Brahmaputra river, originating in the Kailash range at an elevation of about 5300 meters above mean sea level, exhibits a wide range of slope variations throughout its course. The river spans a total length of approximately 2880 kilometres, distributed as follows: 1625 kilometres in Tibet, 918 kilometres in India, and 337 kilometres in Bangladesh before emptying into the Bay of Bengal.

In this study, one year-long (April 2023 to April 2024) time series observation was used near the bank of the river Brahmaputra at Guwahati (26°10'52.90"N, 91°41'49.31"E) as it narrows to 1 km wide here due to down cutting of rocks at Shillong plateau. Seasonal observation was carried out spatiotemporally from July 2022 to June 2024 in tributaries of Brahmaputra, joining the mainstream (Fig. 2). Before the river Brahmaputra enters India, the Tsangpo river takes a prominent curve at Namcha Barwa and continues as river Siang inside India. The right-hand tributary, the Siyom river, joins the Siang river at Komsing Karo, and then it flows till Pasighat finally appears in the plains. Then, after the confluence of two major rivers (Dibang and Lohit) with Siang, it became very wide and called Brahmaputra. With due course as it moves downstream, a few more tributaries join the mainstream, namely Burhi Dihing river, Dihing river, Dhansiri river, and Kopili river from the left bank and from the right bank Subansiri river, Kameng river, Manas river, Sankosh river, and Teesta river join the main stream of the Brahmaputra.

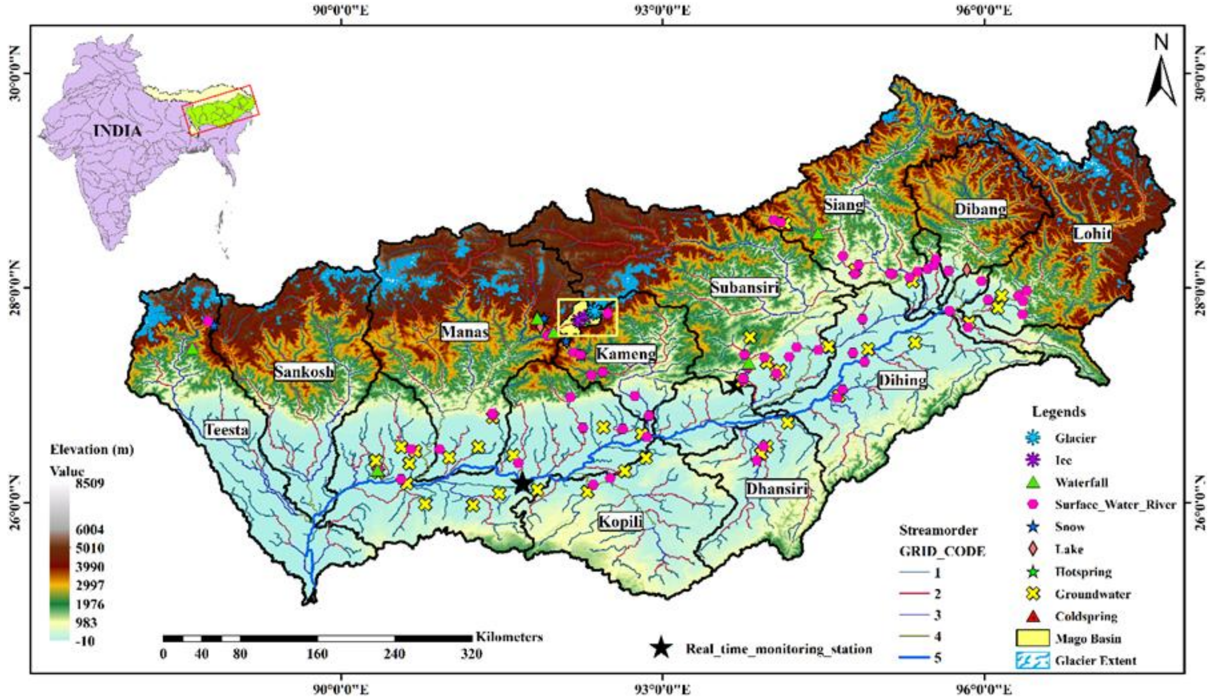

Fig. 2. Topographic map of the Brahmaputra River basin, highlighting tributaries outlined in black. Elevation is depicted using a colour gradient from -10 to 8,509 meters. The river network is categorized by stream order, indicated in various colours. The glacier extent, marked in blue, is derived from the Randolph Glacier Inventory 6.0. Sampling locations and types are clearly indicated on the map's legend.

2.2. Sample collection

The stream water time series samples were collected from a stable barge located 15-20 meters off the northern bank in Guwahati (26°10'54" N, 91°41'49" E) to represent the mainstream of the Brahmaputra river (Fig. 2). River water samples were collected twice a week consistently throughout the entire study period from April 2023 to June 2024. On the same day, groundwater was also collected 2 km away from the bank of Brahmaputra, paying attention to the dates of stream water collection at the exact location named Namati Jalah (26°11'36" N, 91°41'12.34" E) to observe the interplay between surface water and groundwater. Rainwater samples were collected soon after following the rainfall events from the rainfall collection unit established at two locations in the Brahmaputra river basin. One location was in Naharlagun, Itanagar (R2: 27°06'14.64" N, 93°41'418.04" E), representing higher altitude and the other was in Guwahati near the stream water collection point (R1: 26°11'04" N, 91°41'35" E) at the bank of Brahmaputra river. The collection was conducted from October 2022 to June 2024. Apart from the time series sampling at a specific location in the Brahmaputra river basin, seasonal sampling was conducted at multiple locations along the various tributaries. A widespread sampling was carried out to collect water samples from streams, groundwater, waterfalls, springs, and lakes during July 2022. Seasonal sampling was carried out along the few stretches of specific tributaries of the Brahmaputra river.

In addition to both season-specific and time-series sampling in the tributaries and the main channel of the lower Brahmaputra river, glacier and snowmelt samples were collected at Khangeri glacier. The Khangeri glacier is located in Mago basin (Latitude: 27°46'59.3" to 27°48'5.6"N, Longitude: 92°21'18.1" to 92°22'2.4"E) at the north-western extremity of Arunachal Pradesh (Fig. 3). It is a valley-type glacier flowing in a northeast-southwest direction, with an altitude ranging from 5000 to 5500 meters above mean sea level. The glacier's accumulation zone is approximately 6000 meters above the mean sea level on Gori-Chen mountain. The glacier's snout (27°46'59.3"N, 92°21'18.1"E) is situated at an altitude of 4909 ± 2 meters above mean sea level, a few kilometres ahead of a place called Marathang. Seasonal sampling of fresh snow and glaciers was conducted in this region during December 2023, March 2024, April 2024, and June 2024. Additional snow samples were collected from Bumla Pass at Tawang and Lachung at Sikkim. Snow samples were carefully gathered from the uppermost layer of the snowpack, ranging from 10 to 15 centimetres in depth. Additionally, ice samples were collected from the vertical wall, which was exposed near the glacier's snout.

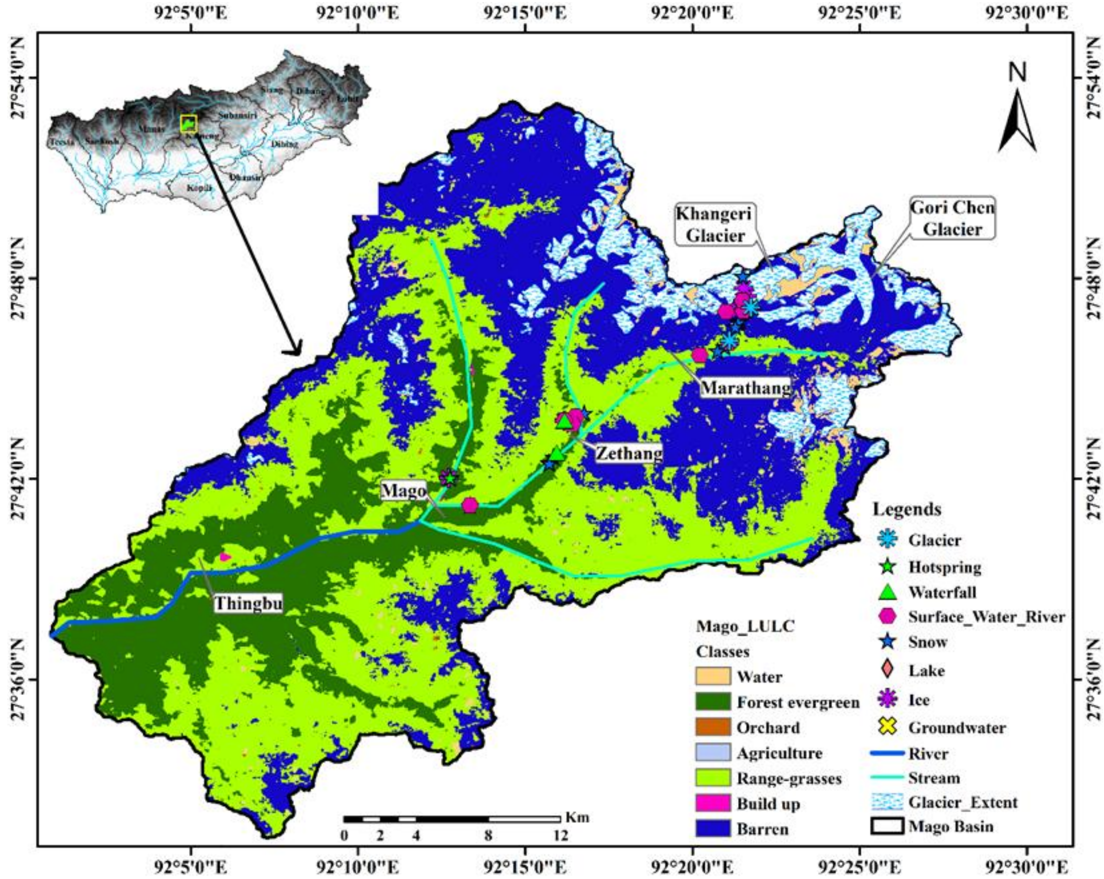

Fig. 3. Topographic map of the Mago basin depicting the Khangeri glacier, where seasonal collections of glacier and snow samples take place. Sampling locations are marked along the glacier's snout, with clear indications of land use, land cover, and the extent of the glacier.

All samples were collected in 15 ml amber narrow-mouth bottles. These bottles were pre-cleaned and acid-washed using 10% reagent-grade hydrochloric acid. Snow and ice samples were collected in previously cleaned plastic zip-lock bags. After melting, the samples were transferred to the amber bottles. The samples were collected underwater with no headspace in the bottle to prevent evaporative fractionation and stored in a place away from sunlight. The samples collected during different times of the year are divided into categories based on the seasons (Fig. 4.). The period from March to May is considered as the pre-monsoon season (Pre-M), while June to September is the monsoon season. The period from October to November is categorised as post-monsoon (Post-M), and December to February is considered as the dry season.

Fig. 4. Field photographs from various sampling locations in the Brahmaputra basin: (a) Snout of the Khangeri glacier in the Mago basin, showing glacier and meltwater sampling; (b) Sampling from the iced lake at Sela Pass; (c) Real-time groundwater sampling in Guwahati; (d) Real-time river water sampling from the Brahmaputra River; (e) Real-time monitoring and sampling of rainfall in Guwahati; (f) Seasonal fresh snow sampling at Bumla Pass, Tawang.

2.3. Stable isotope analysis

This stable isotope analysis was conducted using Liquid Triple Isotopic Water Analyser GLA-431 series based on off-axis integrated cavity output spectroscopy (OA-ICOS) technology developed by Los Gatos Research (LGR), focuses on accurately identifying the stable isotopes of oxygen (O^{16}, O^{17}, and O^{18}) and hydrogen (H^1 and H^2) present in various water types including stream water, groundwater, rain, snow, and ice. The analysis was conducted at the water isotope lab of the Earth System Science and Engineering Division in the Department of Civil Engineering, Indian Institute of Technology Guwahati.

To conduct the analysis, 1 ml of water samples extracted using a 2.5 ml disposable syringe were filtered using the non-sterile Nylon membrane syringe filter with a 0.2 μm pore diameter. The extracted 1 ml water sample will be loaded into a glass vial. The auto-injector system of the analyser will collect 1.2 μl of the sample using a C-line fixed needle syringe and will be introduced into a heated pot locked by a silicon septum. The heated pot is maintained at a temperature of approximately 90°C. The instrument having an optical cavity, kept at vacuum by a diaphragm pump, connected through a PTFE transfer tube. In the heated pot, the water samples will be vaporised and channelised into this optical cavity. This process is carried out at least 10 times for each sample, with the first two injections discarded to eliminate any potential carry-over effects from previous samples. The analysis was carried out following this procedure for all the samples collected.

2.4. Instrument calibration

The isotopic compositions are generally represented by standard delta (δ) notation relative to the international standard VSMOW (Vienna Standard Mean Ocean Water) and expressed in per mil (‰) defined as the Eq. (1) to (3):

$$\delta^{18}O=\left(\frac{\left(O^{18}/O^{16}\right)_{Sample}}{\left(O^{18}/O^{16}\right)_{VSMOW}}-1\right)\times 1000\ ‰ \qquad (1)$$

$$\delta^{17}O=\left(\frac{\left(O^{17}/O^{16}\right)_{Sample}}{\left(O^{17}/O^{16}\right)_{VSMOW}}-1\right)\times 1000\ ‰ \qquad (2)$$

$$\delta^{2}H=\left(\frac{\left(H^{2}/H^{1}\right)_{Sample}}{\left(H^{2}/H^{1}\right)_{VSMOW}}-1\right)\times 1000\ ‰ \qquad (3)$$

The VSMOW given in the above equation is the international standard for δD, $\delta^{18}O$, and $\delta^{17}O$. If VSMOW is not available as standard, the alternate method is used to establish lab standards with respect to VSMOW. Therefore, in this study, standards supplied by LGR, which is calibrated to VSMOW, were used. The calibrated value of lab standards with respect to VSMOW is given in Table 1. Further, three representative samples from this study were analysed at the National Institute of Hydrology, Roorkee, using an Isotopic Ratio Mass Spectrometer (IRMS) as an additional calibration process. In addition to this, three separate samples were further analysed at the Center for Stable Isotope Biogeochemistry, University of California, Berkeley, using the Thermo Delta V Plus mass spectrometer. The absolute differences between the values analysed in both NIH and the University of California, Berkeley, with respect to IIT Guwahati, are given in Table 2. The analytical precision of the L-TIWA GLA 431 series instrument is 0.2 ‰ for δD and 0.02 ‰ for $\delta^{18}O$ and $\delta^{17}O$, which is within the approved limit. Apart from δD, $\delta^{18}O$, and $\delta^{17}O$, d excess was another derived parameter also calculated using the formula (δD – 8 × $\delta^{18}O$) as defined by Dansgaard (1964).

Table 1

Calibrated isotope values of lab standards relative to the VSMOW international standard.

Lab Standard	δD	$\delta^{18}O$	$\delta^{17}O$
LGR 1D	–161.3 ± 0.5 ‰	–20.72 ± 0.15 ‰	–10.93 ± 0.15 ‰
LGR 2D	–120.2 ± 0.5 ‰	–16.13 ± 0.15 ‰	–8.49 ± 0.15 ‰
LGR 3D	–78.0 ± 0.5 ‰	–10.76 ± 0.15 ‰	–5.63 ± 0.15 ‰
LGR 4D	–48.7 ± 0.5 ‰	–7.63 ± 0.15 ‰	–3.97 ± 0.15 ‰
LGR 5D	–10.5 ± 0.5 ‰	–3.0 ± 0.15 ‰	–1.52 ± 0.15 ‰

Table 2

Summary of OA-ICOS and mass spectrometer measurements of various sample types at IIT Guwahati, NIH, and the University of California.

Sample ID	Type of sample	δD	$\delta^{18}O$	δD	$\delta^{18}O$	Absolute difference	
		NIH		IITG		δD	$\delta^{18}O$
GPR	Rainwater	–17.33	–3.47	–17.71	–3.08	0.38	0.39
GSW	River water	–43.66	–7.19	–44.35	–7.47	0.69	0.28
GWG	Groundwater	–33.66	–5.32	–34.17	–5.15	0.51	0.17
		UC Berkeley		IITG			
SWR	River water	–49.6	–7.72	–49.49	–7.71	0.11	0.01
GW	Groundwater	–32.4	–5.81	–32.65	–5.78	0.25	0.03
SP	Spring water	–41.3	–6.23	–40.87	–6.42	0.43	0.19

3. Results and discussion

3.1. Isotopic signature of precipitation

This study analyses the isotopic signatures of precipitation at two sampling sites in the Brahmaputra basin (Guwahati and Itanagar) from October 2022 to June 2024. The isotopic composition of precipitation samples collected from Guwahati exhibited considerable variability in $\delta^{18}O$, $\delta^{17}O$ and δD throughout the study period. The $\delta^{18}O$ values ranged from –14.46 ‰ to 4.09 ‰, with a mean value of –3.18 ‰ (±4.44 ‰), while $\delta^{17}O$ values ranged from –7.75 ‰ to 2.58 ‰, with a mean value of –1.59 ‰ (±2.39 ‰), and δD values ranged from –113.46 ‰ to 40.91 ‰, with a mean of –14.51 ‰ (±37.32 ‰). The d-excess values varied between –3.87 ‰ and 26.70 ‰, with an average of 10.89 ‰ (±5.80 ‰). The isotopic composition of precipitation collected from Itanagar exhibits variability in $\delta^{18}O$ values ranging from –12.89 ‰ to –1.15 ‰, and δD values ranging from –86.53 ‰ to 10 ‰. The d-excess values varied between 13.34 ‰ and 19.21 ‰.

The LMWL displays the linear relationship between $\delta^{18}O$ and δD derived from precipitation at Guwahati and Itanagar as illustrated in Fig. 5. The linear regression equation defining LMWL is given below:

$$\text{LMWL}, \delta D = 8.2387 \times \delta^{18}O + 11.967 \quad (4)$$

The (Eq. (4)) shows a slight deviation in slope and intercept from the universal reference line known as Global Meteoric Water Line, established by Craig (1961). Defined by the equation:

$$\text{GMWL}, \delta D = 8 \times \delta^{18}O + 10 \quad (5)$$

However, Indian Meteoric Water Line by Kumar et al., (2010) in (Eq. (6)) shows a slightly lower slope and intercept than GMWL, illustrated by linear regression equation as:

$$\text{IMWL}, \delta D = 7.93\ (\pm 0.06) \times \delta^{18}O + 9.9\ (\pm 0.5), n = 272, r^2 = 0.98 \quad (6)$$

The Meteoric Water Line (MWL) for the precipitation at Guwahati from October 2022 to July 2024 shows the regression line, defined by the equation:

$$\text{R1}, \delta D = 8.3028 \times \delta^{18}O + 11.848 \quad (7)$$

Seasonal meteoric water lines were also developed to understand the influence of season on the isotopic signature of rainfall. Seasonal differences were notable for precipitation in Guwahati, with Pre-M showing enriched $\delta^{18}O$, $\delta^{17}O$, and δD values (mean $\delta^{18}O$: –0.99 ‰; mean $\delta^{17}O$: –0.52 ‰; mean δD: 3.50 ‰) compared to Post-M (mean $\delta^{18}O$: –11.02 ‰; mean $\delta^{17}O$: –5.81 ‰; mean δD: –79.37 ‰) (Table 3). This seasonal trend was consistent across all sampling locations. The enriched $\delta^{18}O$ shows a higher concentration of heavier oxygen isotope (^{18}O) in the rainwater than the lighter oxygen isotope (^{16}O). Higher concentrations of heavier isotopes reflect in rainwater when there is less prior condensation, local precipitation during dry seasons, or shorter moisture transport distances. The linear regression relation for each season is defined by the equations:

Pre-Monsoon, $\delta D = 8.0717 \times \delta^{18}O + 11.454$ (8)

Monsoon, $\delta D = 8.6569 \times \delta^{18}O + 14.087$ (9)

Post-Monsoon, $\delta D = 6.759 \times \delta^{18}O - 4.8713$ (10)

Dry season, $\delta D = 5.7629 \times \delta^{18}O + 15.241$ (11)

The regression line has a slope closer and intercept greater than GMWL for pre-monsoon samples, but the monsoon samples show a trend line similar to the global meteoric water line and intercept even larger than the pre-monsoon. The smaller intercept difference in the pre-monsoon and monsoon rainwater samples indicates that the moisture sources of precipitation in this region originate from the recycled Indian summer monsoon more than the western disturbances. A higher intercept compared to GMWL shows an evaporative enrichment in precipitation. Post-monsoon samples show a trend line with a negative intercept and lower slope than GMWL, for the reason that the retreating Indian Summer Monsoon transports moisture from a great distance.

The precipitation samples of Itanagar show a regression line similar to the global meteoric water line. The MWL for the precipitation from October 2022 to July 2023 is defined by the equation:

R2, $\delta D = 8.4528 \times \delta^{18}O + 18.055$ (12)

The slope of MWL at Itanagar is comparable to the slope of GMWL. However, the intercept shows a higher value, which could be due to the altitude effect, as Itanagar is at a higher elevation. Therefore, due to the altitude effect, the evaporative vapour under low humidity conditions shows a selective loss of lighter isotopes, resulting in an increase in d-excess. Like in Guwahati, the pre-monsoon rainfall shows enrichment in heavier isotope signatures due to the notable influence of evaporation during pre-monsoon. Post-monsoon rainfall shows depletion in heavier isotope signatures due to the influence of retreating moisture transportation during post-monsoon.

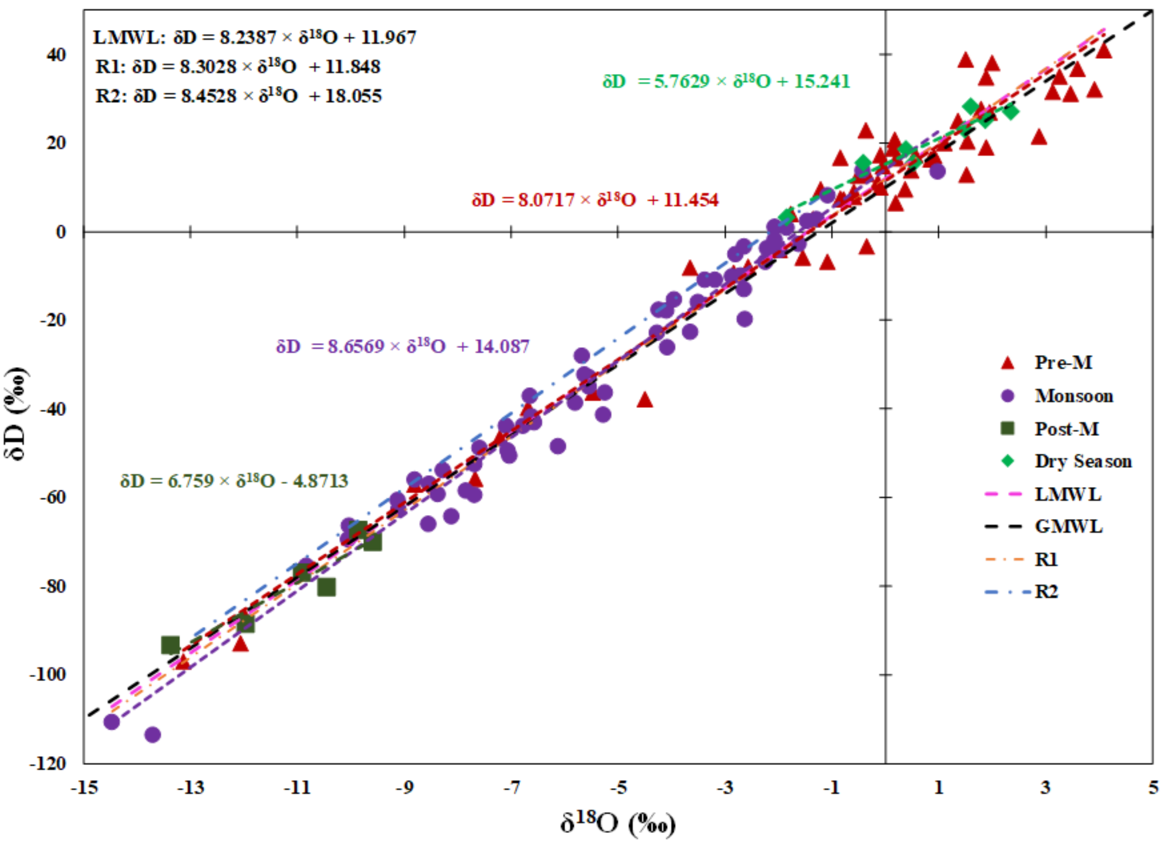

Fig. 5. Relationship between $\delta^{18}O$ and δD values in precipitation samples from Guwahati and Itanagar, illustrating isotopic variation in the Brahmaputra river basin at differing elevations. The pink dotted line represents the Local Meteoric Water Line (LMWL), while the Global Meteoric Water Line (GMWL) is provided in black dotted line for comparison. The linear trend lines, R1 and R2, correspond to precipitation at Guwahati and Itanagar, respectively. Seasonal variations, including pre-monsoon, monsoon, post-monsoon, and dry-season influences, are depicted through the scatter of data points and the trend lines.

Table 3

Summary of isotopic precipitation data by season in Guwahati: mean, median, range, and standard deviation.

Season	Isotopes	Mean	Median	Range	Standard Deviation
Pre-M	δ^{18}O	–0.99‰	–0.10‰	–13.12‰ to 4.09‰	±3.86‰
	δ^{17}O	–0.52‰	–0.13‰	–6.94‰ to 2.58‰	±2.13‰
	δD	3.50‰	12.84‰	–97.01‰ to 40.91‰	±31.85‰
Monsoon	δ^{18}O	–5.08‰	–4.76‰	–14.46‰ to 0.97‰	±3.15‰
	δ^{17}O	–2.48‰	–2.37‰	–7.75‰ to 0.55‰	±1.78‰
	δD	–30.50‰	–27.04‰	–113.46‰ to 13.79‰	±28.19‰
Post-M	δ^{18}O	–11.02‰	–10.68‰	–13.37‰ to –9.59‰	±1.30‰
	δ^{17}O	–5.81‰	–5.57‰	–7.14‰ to –4.97‰	±0.74‰
	δD	–79.37‰	–78.55‰	–93.33‰ to –67.28‰	±9.27‰
Dry season	δ^{18}O	0.75‰	1.01‰	–1.84‰ to 2.35‰	±1.29‰
	δ^{17}O	0.47‰	0.49‰	–0.88‰ to 1.71‰	±0.77‰
	δD	19.55‰	20.77‰	3.12‰ to 28.24‰	±7.74‰

A time series from October 2022 to June 2024 for δ^{18}O and d-excess were plotted (Fig. 6) to understand the localised recycling of moisture. During pre-monsoon, the mean of δ^{18}O, δ^{17}O, and δD is less negative, indicating enrichment in isotopic signature along with highly enriched d-excess and high standard deviation (Table 3, Fig. 6). The enriched values indicate the gradual increase in temperatures and lower humidity levels typically experienced during the summer season due to localised recycling dominance. Ganguly et al. (2023) have reported a similar kind of trend in Jorhat due to locally recycled moisture dominance. This suggests a notable influence of evaporative processes. This evaporation enriches moisture with the heavier isotope, contributing to isotopically enriched rainfall. This region often experiences convective thunderstorms during the pre-monsoon period, causing rapid uplift of the moisture. This uplifted moisture sometimes leads to intense and short-duration rain events and can vary widely across different storms, resulting in higher variability in standard deviation in isotopic signature.

The isotopic signature for the monsoon season shows a wide range from negative to positive, with a high standard deviation in Table 3. This variation is attributed to several reasons, including complex hydrological dynamics in the Brahmaputra river basin. It receives moisture from the southwest monsoon, the Arabian sea, and recycled continental moisture during the mid-monsoon period (Fig. 6). Each source has a different isotopic signature. Intense monsoon events also lead to heavy rainfall, resulting in more significant isotopic depletion. A baseline shift in $\delta^{18}O$ was observed with the depleting trend of monsoon trend around mid-June (Fig. 6). The intensity of rainfall, for this reason, varies greatly, from short downpours for a prolonged period to heavy rain for a short period, contributing to a wide range of variations. Also, early monsoon rains generally undergo less rainout, resulting in precipitation of heavier isotopes first than peak and late monsoon rains. While later rains after extensive pouring show a more depleted signature. Laskar et al. (2015) and Ganguly et al. (2023) also have reported a gradual depletion of isotopic composition with the due course of monsoon season at Hailakandi and Jorhat in Assam, respectively.

The isotopic signature for the precipitation in the post-monsoon season indicates a transition from monsoon to dry season shown by depletion in heavier isotopes. This could be attributed to the combined effect of retreating ISM moisture and the impact of cooler mid-latitude western disturbances. According to Jeelani et al. (2018), heavy isotope depletion is observed in north-eastern India due to the transition of moisture sources from the Indian Summer Monsoon to the western disturbances period. The depletion in heavier isotopes occurs due to the isotopic fractionation of water vapour as it travels from oceans or other large water bodies over a long distance, and the cold temperature causes progressive loss of heavier isotopes due to condensation.

Among the four seasons, the mean of all the isotopic fractionations shows a positive signature during the dry season because of specific reasons listed: (1) local recycled moisture sources, (2) reduced rainout effect, or (3) lesser precipitation amount. As this region experiences dry winters, there is more influence from recycled moisture that has been previously evaporated and re-precipitated (Fig. 6). Since the local moisture has not travelled from a greater distance, it retains a higher concentration of the heavier isotopes. In contrast to the monsoon season, the drier season experiences less fractionation as there are no repeated precipitation events to deplete heavier isotopes due to the rainout effect. Rainfall is often lower in volume and less frequent during the dry season, which leads to less dilution of heavier isotopes by subsequent rainfalls, showing isotopic enrichment. The standard deviations indicate less significant variability in isotopic values during the dry season compared to Pre-M, monsoon and Post-M, reflecting the influence of changing weather patterns, moisture sources, altitude effects, and rainout events.

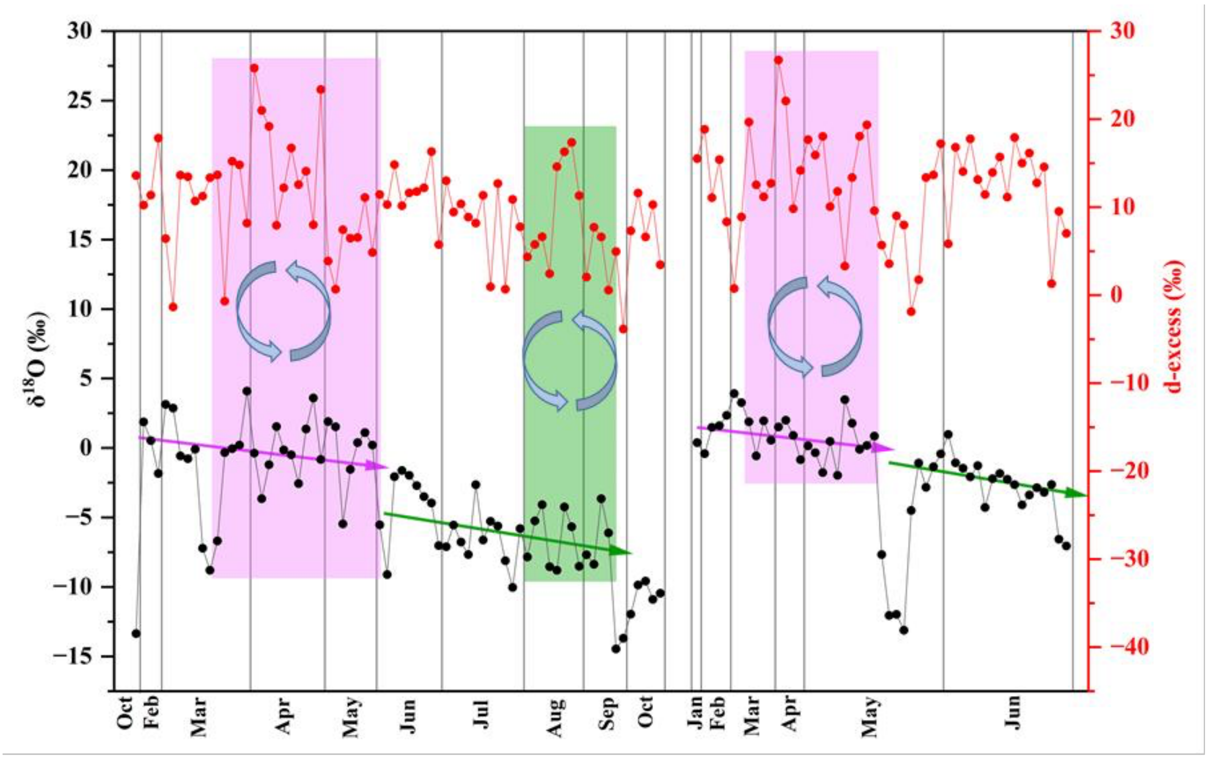

Fig. 6. Isotopic signature of $\delta^{18}O$ and d-excess shows the trend of daily precipitation in Guwahati from October 2022 to June 2024. The pre-monsoon period (March to May) displays enriched $\delta^{18}O$ and d-excess values. The shift in $\delta^{18}O$ during the later part of the Indian Summer Monsoon (June to September) reflects contributions from localized recycled moisture. The pink rectangle represents the pre-monsoon recycled moisture zone, while the green rectangle represents the monsoon-recycled moisture zone.

The results reveal distinct seasonal variations in isotopic composition, with $\delta^{18}O$ and δD values showing significant enrichment during the pre-monsoon season and depletion during the post-monsoon season. In the study area, it was found that a considerable difference in isotopic signatures between the high-altitude location at Itanagar and the low-altitude location at Guwahati. This suggests that altitude has an impact on isotopic enrichment. Also, correlations between isotopic ratios and atmospheric circulation patterns were observed, which gave insights into regional moisture sources.

The correlation between $\delta^{18}O$ and d-excess values and various meteorological parameters, including precipitation amount (mm/day), temperature, and relative humidity at 2 meters indicate a strong and statistically significant relationship emphasising a strong atmospheric interference in hydrological cycle (Fig. 7). Temperature is showing strongly positive correlation with $\delta^{18}O$ values, the enriched isotopic values observed in the month of March-April shows increasing trend of temperature but precipitation amount are less. Precipitation negatively correlates with the isotopic composition in $\delta^{18}O$ values. Higher precipitation amounts are associated with depleted isotopic values due to the incorporation of moisture from distant sources. Relative humidity shows a weak positive correlation with d-excess.

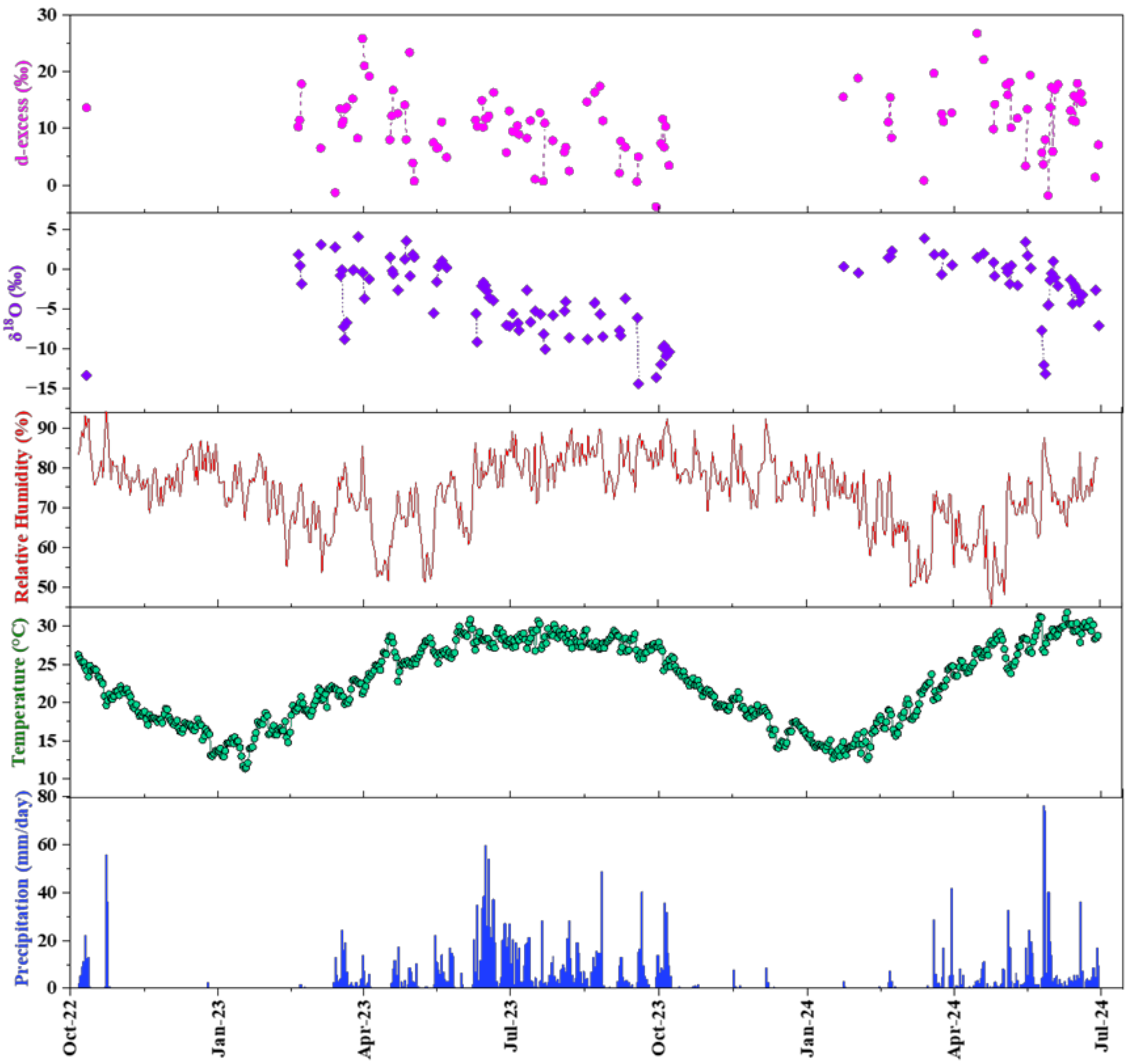

Fig. 7. Plot shows temporal variation of the isotopic signature of precipitation ($\delta^{18}O$ and d-excess) and its relationship with meteorological variables at the Guwahati station. The data, sourced from NASA/POWER CERES/MERRA2, presents daily measurements of precipitation amount (mm/day), relative humidity at 2 meters (%), and earth skin temperature (°C).

3.2. Isotopic signature of snow and glacier

Snow and glacier samples were collected during different seasons for isotopic analysis. Systematic seasonal sampling was carried out at Khangeri Glacier during April 2024 and June 2024. Systematic snow sampling was done from Khangeri glacier in the Mago basin during

December 2023 and April 2024. Additionally, snow samples were collected from Bumla pass during December 2022 and March 2023 and from Lachung at Sikkim during March 2024.

The $\delta^{18}O$ and δD values in snow vary from –6.43 ‰ to 1.44 ‰ and –32.94 ‰ to 40.66 ‰, respectively, for pre-monsoon season and –24.54 ‰ to –16.27 ‰ and –180.36 ‰ to –105.80 ‰, respectively for dry season. The glacier isotopic signature (varies in $\delta^{18}O$ –17.20 ‰ to –12.62 ‰ and δD –112.35 ‰ to –87.70 ‰) shows intermediate composition with more nearly to dry season snow composition and does not vary much according to the season. Dry-season snow shows a depleted isotopic signature compared to pre-monsoon, which indicates melting is triggered due to highly humid conditions and more evaporation. The $\delta^{18}O$ and δD relationship in Fig. 8 shows that the overall isotopic signature of snow above the GMWL and glacier lies along the global meteoric water line. The linear regression relationship for pre-monsoon snow shows a slope similar to GMWL with a higher intercept (Eq. (13)); however, the snow from the dry season shows a higher slope and intercept, as shown in Eq. (14). The regression line for glacier shows a slope lower than GMWL and a negative intercept, defined by the Eq. (15):

Pre-monsoon, $\delta D = 8.1803 \times \delta^{18}O + 24.819$ (13)

Dry season, $\delta D = 9.2849 \times \delta^{18}O + 50.058$ (14)

Glacier, $\delta D = 6.678 \times \delta^{18}O - 6.0761$ (15)

The negative intercept in the glacier regression line indicates rapid changes in temperature, which is one of the main hydro-meteorological variables that causes glacier melting. This often reflects secondary fractionation processes due to distinct climatic impacts on hydro-meteorological parameters and the mixing of precipitated water and melted water within the glacier. Also, it is indicative of local climate changes impacting the glacier's isotopic composition.

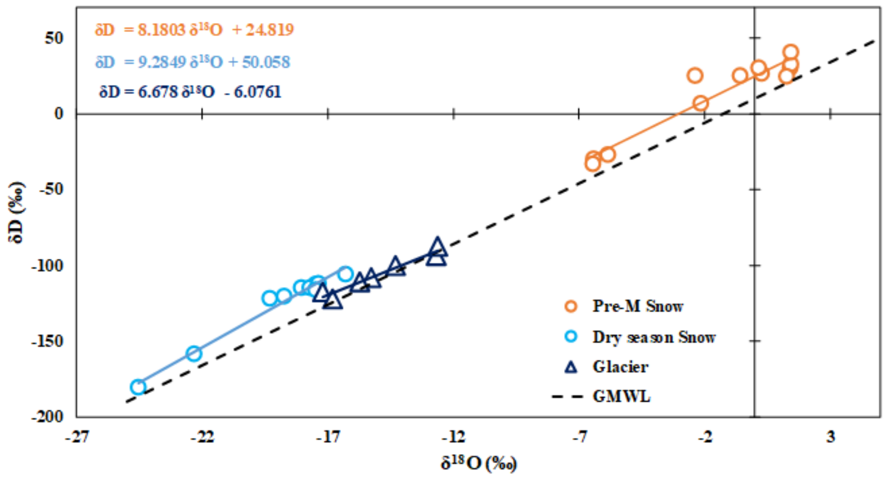

Fig. 8. The plot showing the relationship between $\delta^{18}O$ and δD isotopic variations in snow and glacier samples from the Brahmaputra river basin.

3.3.Temporal isotopic signature of Brahmaputra river at Guwahati

This study analyses temporal variability in isotopic signature for Brahmaputra river water for the duration of April 2023 to June 2024 at Guwahati. It exhibits considerable temporal variability in $\delta^{18}O$, $\delta^{17}O$, and δD throughout the study period. The $\delta^{18}O$ values ranged from –11.88 ‰ to –6.54 ‰, with a mean value of –9.27 ‰ (±1.25 ‰), while $\delta^{17}O$ values ranged from –6.10 ‰ to –3.25 ‰, with a mean value of –4.88 ‰ (±0.63 ‰), and δD values ranged from –78.99 ‰ to –32.65 ‰, with a mean of –59.49 ‰ (±11.52 ‰). The d-excess values varied between 7.81 ‰ and 22.44 ‰, with an average of 14.94 ‰ (±2.68 ‰).

It is observed from Table 4. that there is less variation in the isotopic signature of Brahmaputra water from season to season except in the dry season. However, the clustering in Fig. 9 shows more enrichment in pre-monsoon and more depletion in post-monsoon. The pre-monsoon regression line is illustrated by the equation given below:

Pre-monsoon, $\delta D = 9.2496 \times \delta^{18}O + 26.3$ (16)

where the slope is a little bit higher than the monsoon, post-m, and dry seasons (Fig. 9). This indicates that the river water has undergone significant interaction with the local moisture circulation or evaporation processes. Also, if there is precipitation or condensation from already recycled moisture due to high humidity conditions, then a higher d-excess is significant. The pre-monsoon river water samples are more enriched than the monsoon samples due to the mixing of precipitation in the upper elevation of the river, which depletes the monsoon signature. The linear regression equation for river water in monsoon, post-monsoon, and dry season is defined by $\delta^{18}O$ and δD relation (Eq. (17) to (19)) are given below:

$$\text{Monsoon, } \delta D = 8.92 \times \delta^{18}O + 23.746 \quad (17)$$

$$\text{Post-monsoon, } \delta D = 8.8043 \times \delta^{18}O + 21.364 \quad (18)$$

$$\text{Dry season, } \delta D = 6.0599 \times \delta^{18}O - 6.1468 \quad (19)$$

The best-fit regression line of surface water river, termed as River Water Line (RWL) is defined by the equation:

$$\text{RWL, } \delta D = 9.0433 \times \delta^{18}O + 24.302 \quad (20)$$

The negative d-excess in the trend line indicates a limited inflow of water as precipitation enters the river system and the evaporative process increases heavier isotopic value, resulting in depletion in d-excess.

Table 4

Summary of isotopic river water data by season in Guwahati: mean, median, range, and standard deviation.

Season	Isotopes	Mean	Median	Range	Standard Deviation
Pre-M	$\delta^{18}O$	–8.16‰	–8.17‰	–9.37‰ to –6.82‰	±0.70‰
	$\delta^{17}O$	–4.43‰	–4.33‰	–5.45‰ to –3.69‰	±0.45‰
	δD	–49.19‰	–50.17‰	–59.96‰ to –32.56‰	±6.81‰

Season	Isotopes	Mean	Median	Range	Standard Deviation
Monsoon	$\delta^{18}O$	–9.47‰	–9.49‰	–11.88‰ to –6.54‰	±1.25‰
	$\delta^{17}O$	–4.92‰	–5.01‰	–6.10‰ to –3.25‰	±0.71‰
	δD	–60.68‰	–59.93‰	–77.15‰ to –35.86‰	±11.27‰
Post-M	$\delta^{18}O$	–10.73‰	–10.61‰	–11.51‰ to –10.45‰	±0.30‰
	$\delta^{17}O$	–5.29‰	–5.22‰	–5.99‰ to –4.97‰	±0.30‰
	δD	–73.08‰	–71.70‰	–78.99‰ to –70.42‰	±2.78‰
Dry season	$\delta^{18}O$	–9.68‰	–9.71‰	–10.68‰ to –8.01‰	±0.65‰
	$\delta^{17}O$	–5.27‰	–5.24‰	–5.96‰ to –4.26‰	±0.45‰
	δD	–64.83‰	–64.32‰	–72.54‰ to –56.28‰	±4.05‰

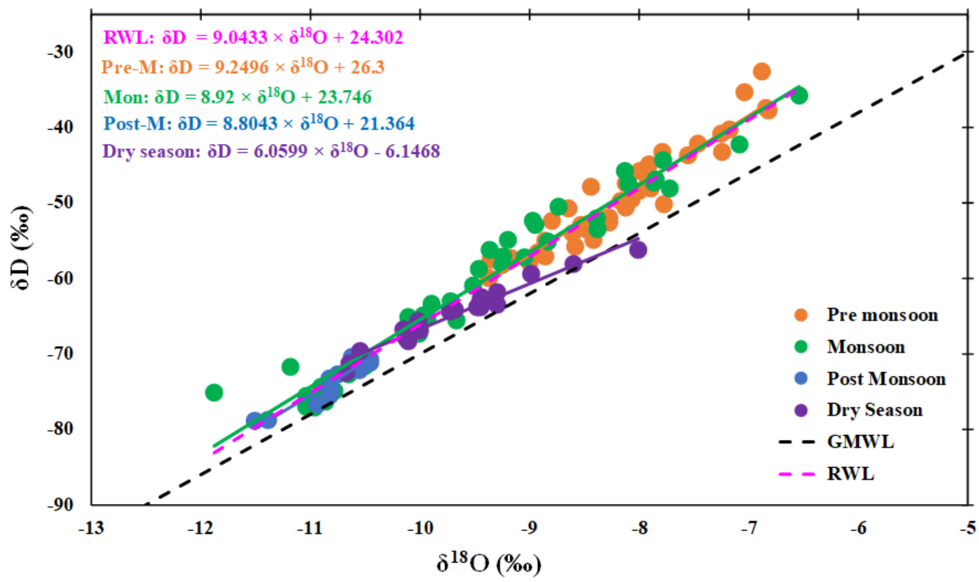

Fig. 9. The scatter plot showing the relationship between $\delta^{18}O$ and δD values in river water samples from Guwahati, illustrating temporal isotopic variations in the Brahmaputra river basin at lower elevations. The pink dotted line represents the River Water Line (RWL), contrasted with the Global Meteoric Water Line (GMWL). Seasonal variations are evident in the scatter of data points, which correspond to the pre-monsoon, monsoon, post-monsoon, and dry seasons.

3.4. Spatial isotopic signature of Brahmaputra river and its tributaries

To study the spatial variation of isotopic signature in the Brahmaputra river, stream water samples were collected form its tributaries. The stable isotopic data for the Brahmaputra river and its tributaries was collected from July 2022– July 2024. The isotopic ratio of $\delta^{18}O$, $\delta^{17}O$, δD, and d-excess ranges from –15.45 ‰ to –4.84 ‰ (mean: –8.94 ‰), –8.51 ‰ to –2.59 ‰ (mean: –4.72 ‰), –112.67 ‰ to –27.68 ‰ (mean: –56.53 ‰), and 8.74 ‰ to –22.52 ‰ (mean: 15.01 ‰) respectively. The spatial variation of $\delta^{18}O$ is illustrated in Fig. 10. Similarly, the spatial variation in $\delta^{17}O$ and δD is illustrated in Fig. 11 and 12, respectively, along the river Brahmaputra and its tributaries, clearly depicting substantial change across different sub-basins. The observation indicates highly depleted isotopic signatures at higher mountainous regions of the Mago basin. As the Mago basin contains glaciers and receives snowfall, the river water in this basin shows the most depletion signature. A significant enrichment trend is observed from the upstream to the downstream part of the river in each sub-basin only after the confluence of streams at several places observed a break in this trend. The confluence scenario completely depends upon the mixing tributary river's isotopic composition. First-order streams in the basin are the primary controller of the isotopic composition of the main channel of the river. Snow/glacier melt-originated first-order streams show a highly negative isotopic composition than the rainwater-generated first-order streams. Also, rainwater generated first-order streams at higher reaches show higher depletion than lower reaches. Mixing of isotopically more negative streams shows a progressive decrease in isotopic signature.

A significant negative correlation was observed in spatial variation of d-excess with other isotopic signatures as illustrated in Fig. 13. Higher mountainous region shows high d-excess indicating enrichment in heavier isotopes. Also, snow/glacier melt-originated first-order streams show highly positive d-excess values than the rainwater-generated first order streams, and rainwater generated first-order streams at higher reach show higher enrichment than lower reaches. The d-excess value of river Brahmaputra at a lower reach a lower value than at a higher reach within the basin.

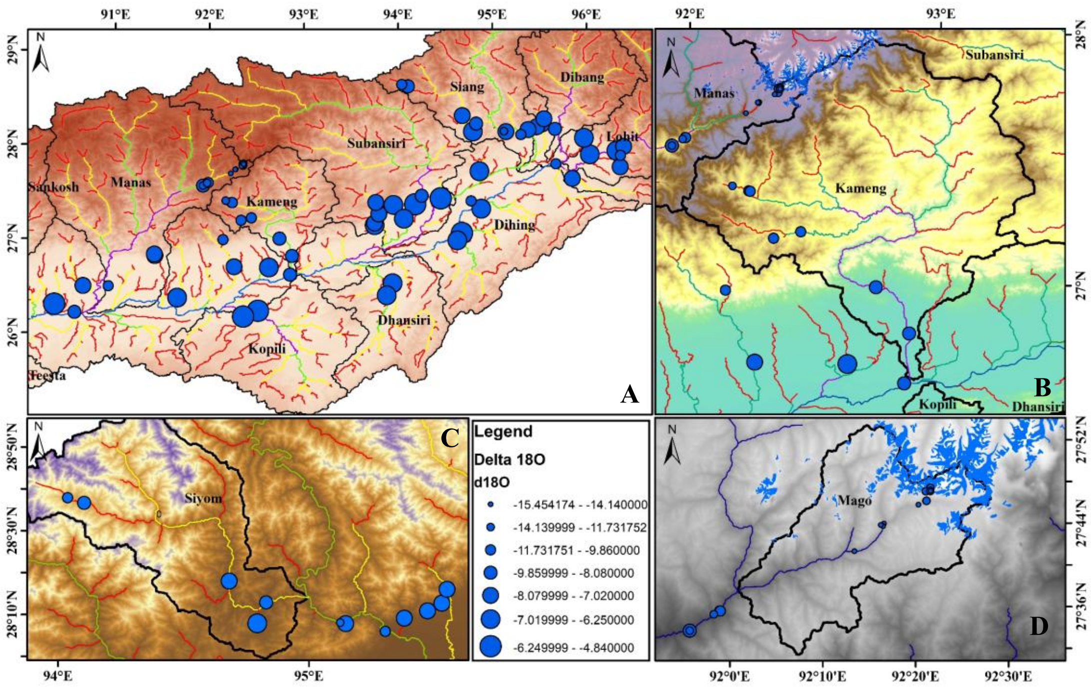

Fig. 10. The map showing the spatial variation in $\delta^{18}O$ for the (A) Lower Brahmaputra basin and its tributaries, (B) Kameng basin, (C) Siyom basin, and (D) Mago basin.

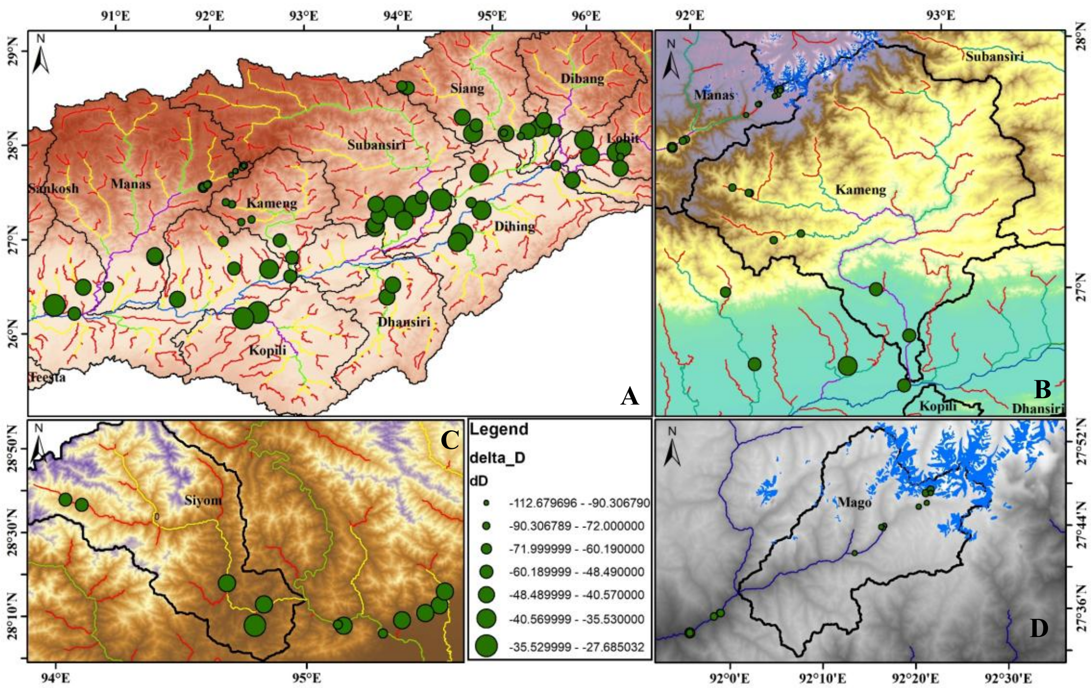

Fig. 11. The map showing the spatial variation in δD for the (A) Lower Brahmaputra basin and its tributaries, (B) Kameng basin, (C) Siyom basin, and (D) Mago basin.

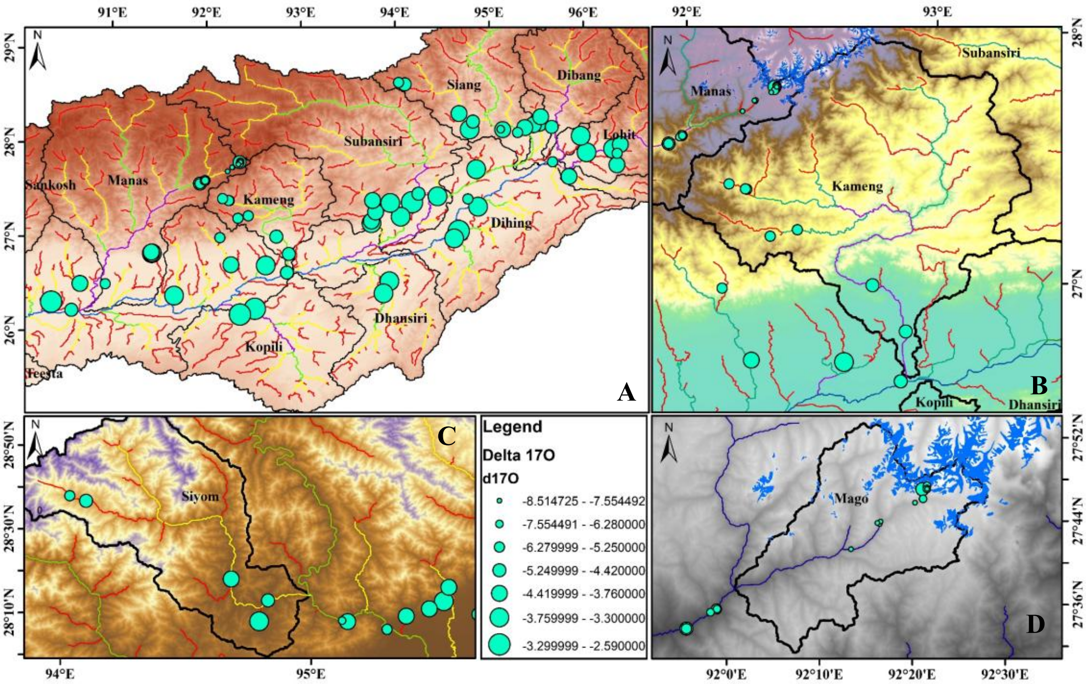

Fig. 12. The map showing the spatial variation in $\delta^{17}O$ for the (A) Lower Brahmaputra basin and its tributaries, (B) Kameng basin, (C) Siyom basin, and (D) Mago basin.

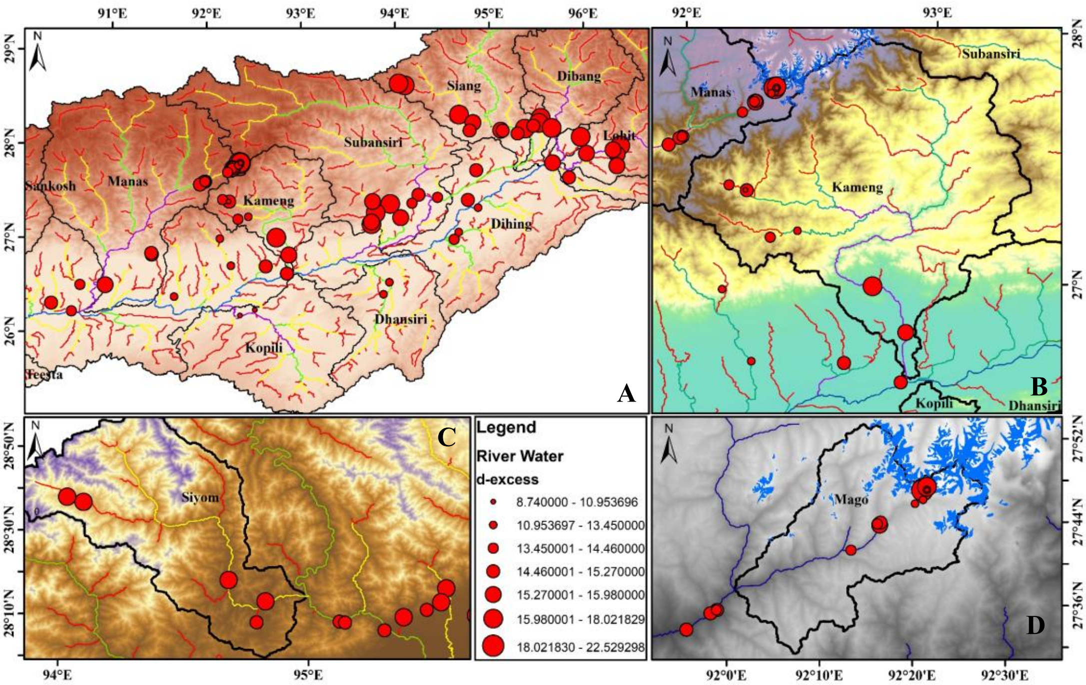

Fig. 13. The map showing the spatial variation in d- excess for the (A) Lower Brahmaputra basin and its tributaries, (B) Kameng basin, (C) Siyom basin, and (D) Mago basin.

3.5.Isotopic signature of groundwater

The study analyses the time series isotopic signature of groundwater in Guwahati from April 2023 to June 2024. Temporal variation of shallow groundwater at Guwahati exhibited considerable variability in $\delta^{18}O$, $\delta^{17}O$, and δD throughout the study period. The $\delta^{18}O$ values ranged from –6.32 ‰ to –4.31 ‰, with a mean value of –5.4 ‰ (±0.38 ‰), while $\delta^{17}O$ values ranged from –3.92 ‰ to –1.01 ‰, with a mean value of –2.85 ‰ (±0.53 ‰), and δD values ranged from –39.41 ‰ to –29.38 ‰, with a mean of –32.90 ‰ (±1.62 ‰). The d-excess values varied between 7.19 ‰ and 14.93 ‰, with an average of 11.21 ‰ (±1.36 ‰).

The results reveal distinct seasonal variations in isotopic composition as shown in Fig. 14 and Table 5, with $\delta^{18}O$ and δD values showing significant sifting in the pre-monsoon trend line to the right of GMWL with correlation equation of

Pre-monsoon, $\delta D = 2.9225 \times \delta^{18}O - 17.092$ (21)

Monsoon, $\delta D = -0.0646 \times \delta^{18}O - 33.155$ (22)

Post monsoon, $\delta D = 9.3554 \times \delta^{18}O + 16.005$ (23)

Dry season, $\delta D = 1.2324 \times \delta^{18}O - 25.48$ (24)

The monsoon trend line indicates significant evaporation, possibly from surface water bodies or soil moisture before or during infiltration. The depleted intercept combined with the more negative slope reflects that the recharge water might travel from a higher altitude or recharged during early monsoon with the impact of colder temperatures. The best-fit regression line developed from $\delta^{18}O$ and δD plot going across GMWL, as shown in Fig. 14, is termed as Groundwater Line (GWL) defined by the equation:

GWL, $\delta D = 1.6859 \times \delta^{18}O - 23.797$ (25)

Table 5

Summary of isotopic groundwater data by season in Guwahati: mean, median, range, and standard deviation.

Season	Isotopes	Mean	Median	Range	Standard Deviation
Pre-M	$\delta^{18}O$	–5.21‰	–5.39‰	–5.82‰ to –4.32‰	±0.44‰
	$\delta^{17}O$	–2.91‰	–2.85‰	–3.70‰ to –2.19‰	±0.37‰
	δD	–32.31‰	–32.08‰	–35.63‰ to –29.38‰	±1.69‰
Monsoon	$\delta^{18}O$	–5.50‰	–5.40‰	–6.33‰ to –4.91‰	±0.42‰
	$\delta^{17}O$	–2.74‰	–2.74‰	–3.89‰ to –1.02‰	±0.68‰
	δD	–32.86‰	–32.69‰	–36.24‰ to –31.09‰	±0.96‰
Post-M	$\delta^{18}O$	–5.45‰	–5.44‰	–5.78‰ to –5.24‰	±0.16‰
	$\delta^{17}O$	–2.74‰	–2.81‰	–3.65‰ to –1.94‰	±0.52‰
	δD	–34.99‰	–34.16‰	–39.42‰ to –33.24‰	±1.76‰
Dry season	$\delta^{18}O$	–5.53‰	–5.53‰	–5.77‰ to –5.27‰	±0.10‰
	$\delta^{17}O$	–3.09‰	–3.08‰	–3.93‰ to –1.93‰	±0.40‰
	δD	–32.30‰	–32.60‰	–33.41‰ to –31.21‰	±0.64‰

Form Fig. 14 it is observed that the pre-monsoon samples are plotted across the GMWL and follows the evaporation trend. The evaporation process causes an overall enrichment in heavier isotopes in the groundwater system. However, deuterium enrichment is low due to the fact that groundwater system has less interaction with the atmospheric water compared to surface water. The isotopic signature of groundwater reflects various processes in the subsurface. The $\delta^{18}O$ and δD relationship in pre-monsoon indicates more fractionation of oxygen isotope due to evaporation. The regression line in monsoon season cutting across the GMWL, which indicates various underground processes, may alter the isotopic composition of groundwater, which gives insights into its subsurface evolution history and geochemical reactions of groundwater while through the soil. Groundwater shows positive $\delta^{18}O$ shifts of varying degrees. This is attributed to the leaching of soil, while recharge from surface water. This usually has no evident effect on δD is due to the lack of hydrogen in most rock-forming minerals and soil particles. The trend line equation for post-monsoon shows higher slope and positive intercept which reflects especially high humid condition and less fractionation during the condensation process. Also shows that the air masses that bring rain have travelled from a large water body and retained significant moisture in it during the recharge.

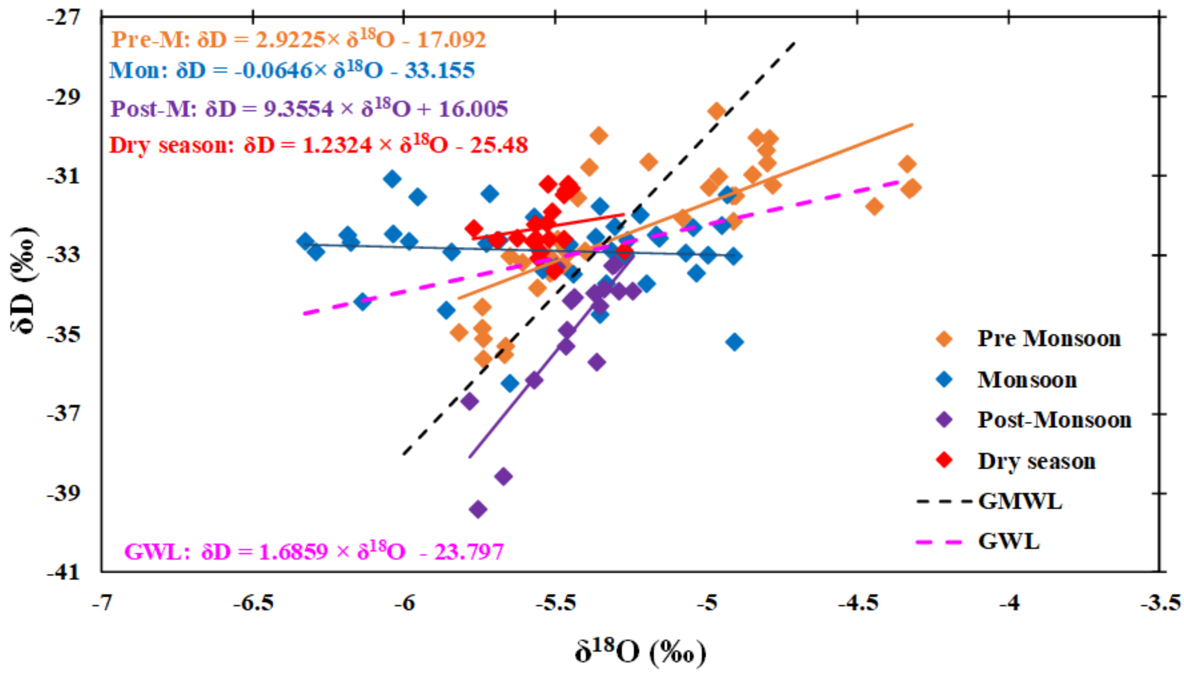

Fig. 14. Relationship between $\delta^{18}O$ and δD values in groundwater samples from Guwahati, highlighting temporal isotopic variation of groundwater in the Brahmaputra river basin. The pink dotted line represents the Ground Water Line (GWL), compared to the Global Meteoric Water Line (GMWL). The scatter of data points reflects seasonal variations, including influences from the pre-monsoon, monsoon, post-monsoon, and dry seasons.

The spatial variation of isotopic signature (δ^{18}O and δD) in groundwater ranged from –8.22 ‰ to –2.63 ‰ (mean: –5.69 ‰) and –52.87 ‰ to –7.99 ‰ (mean: –33.05 ‰) respectively. Fig. 15 shows δ^{18}O spatial variation in groundwater along the reach of the Brahmaputra river and its tributaries. The variation shows relatively more negative isotopic composition with decreasing distance from lower-order streams. Decreasing distance from higher order streams shows enriched signature. The groundwater locations near the main trunk of the Brahmaputra river show relatively less negative value. In most cases, the groundwater isotopic composition depends upon its recharge characteristics and the presence of surface water for interaction.

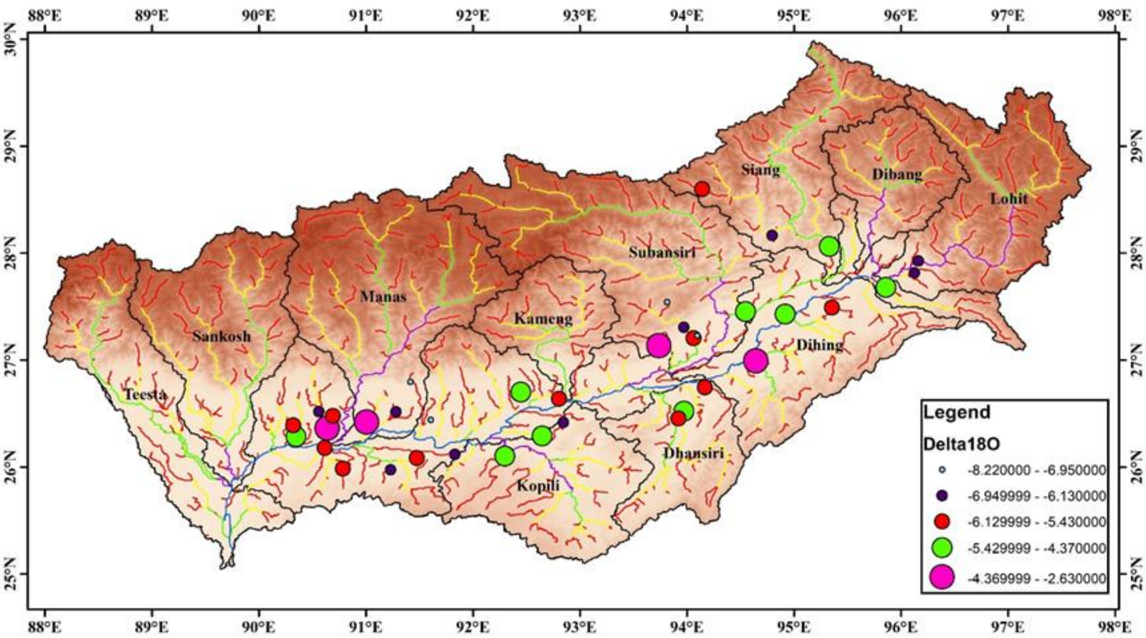

Fig. 15. The map showing the spatial variation of the groundwater in δ^{18}O for the Brahmaputra river basin.

4. Conclusions

The present study has investigated the trends in the isotopic signature for seasonal and annual precipitation at two locations (Guwahati and Itanagar) from October 2022 to July 2024. The trend line intercept is higher in Itanagar than in Guwahati due to the continental or altitude effect. The seasonal analysis shows that pre-monsoon precipitation shows an enriched signature while post-monsoon shows depletion. Meanwhile, the monsoon isotopic signature range shows a high standard deviation. Monsoon precipitation largely caused by oceanic moisture influx, increases surface water availability in the Brahmaputra basin due to floods in low-lying floodplains and wetlands, resulting in enhanced moisture recycling, especially in the late monsoon period.

Further, the characteristics of hydrological processes in the Brahmaputra river system were assessed using stable isotopes. Distinct isotopic trends were observed along the course of the river, reflecting the effect of local climate scenarios, physiography, and difference in the source of water. The river water from the upstream mountainous region depicts a highly depleted isotopic signature. Along the course of the Brahmaputra river, a systematic trend is observed due to enriched isotopic signature in the downstream direction. Similarly, an enrichment in d-excess value is observed at the upstream part of the river, displaying a decreasing trend in the downstream direction. Further, along the main channel of the Brahmaputra river in the downstream direction, isotopic variability was low, indicating stabilisation within a narrow range of $\delta^{18}O$: –6.24 ‰ to –4.84 ‰. Temporal isotopic variability in the river water indicates an enriched signature in pre-monsoon and a depleted signature in post-monsoon.

The spatial and temporal distribution of isotopic signatures in groundwater is controlled by the recharge source. Temporal variation in the shallow aquifer exhibits an evaporative trend in pre-monsoon and dry season, indicating either pre or post-recharge evaporation. Meanwhile, the monsoon trend shows large variability in $\delta^{18}O$ indicating the complexities in recharge through the soil from meteoric water. The post-monsoon regression line is slightly below the GMWL indicating mixing of the older groundwater with the newer meteoric water.

The spatio-temporal isotopic variability in river water is distinct due to different hydrological processes such as altitude effect, evaporative enrichment, sources of water, and mixing with tributaries. Precipitation is the main contributor of surface water and groundwater within the

Brahmaputra river system. The seasonal isotopic trend of precipitation indicates the contribution of moisture from three sources: the Indian Summer Monsoon originating from the Bay of Bengal, the southwest monsoon from the Arabian Sea, and the westerlies from the Mediterranean Sea. The first-order streams from glacierised basin show a highly negative isotopic composition than the first-order streams of non glacierised basin. This difference in isotopic signatures is primarily due to the distinct sources of water. Streams contributed by snow melts and glaciers exhibit a significantly more negative isotopic composition than streams contributed by rainfall. The mixing of river water from several sources in the Brahmaputra river system, mainly from tributaries at confluences, showed relatively enriched isotopic values in the downstream direction of the river. Therefore, the spatiotemporal variability in the isotopic signature in the Brahmaputra river system clearly demonstrates the imprints of various hydrological processes within the water cycle. The findings from this study created a better knowledge on the hydrological behaviour of the Brahmaputra river system. Such studies can be utilised in taking appropriate measures for the crucial management of water resources and predicting climate change impacts on river systems.

Acknowledgement

The authors express their heartiest gratitude to the Department of Science and Technology (DST), Government of India (Project No – DST/CCP/MRDP/185/2019) under DST–SPLICE–Climate change program for funding the high-precision laser-based Liquid Triple Isotopic Water Analyser (used in this study). Special thanks to Professor Suresh A. Kartha for the successful completion of several field visits to different parts of the Brahmaputra basin. The authors are grateful to Ms. Tashi Yangjom, the woman Mount Everest summiteer of 2021, for helping in the glacier sample recovery from the Khangeri glacier. The first author acknowledges the help from the National Institute of Mountaineering and Allied Sports (NIMAS, Dirang) for the trekking to Khangeri glacier. This research was supported by the

Prime Minister's Research Fellowship to Madhusmita Nanda (PMRF ID: 1900816), funded by the Ministry of Education, Government of India.

References

Aggarwal, S.P., Thakur, P.K., Nikam, B.R., Garg, V., Chouksey, A., Dhote, P.R., Bisht, S., Dixit, A., Arora, S., Choudhury, A., Sharma, V., 2020. Role of earth observation data and hydrological modeling in supporting un SDGS in North West Himalaya. The International Archives of the Photogrammetry, Remote Sensing and Spatial Information Sciences 43, 853-860.

Banda, L.C., Kalin, R.M., Phoenix, V., 2024. Isotope hydrology and hydrogeochemical signatures in the Lake Malawi Basin: a multi-tracer approach for groundwater resource conceptualisation. Water 16(11), 1587.

Bershaw, J., Penny, S.M., Garzione, C.N., 2012. Stable isotopes of modern water across the Himalaya and eastern Tibetan Plateau: Implications for estimates of paleoelevation and paleoclimate. Journal of Geophysical Research: Atmospheres 117(D2).

Bookhagen, B., Burbank, D.W., 2010. Toward a complete Himalayan hydrological budget: Spatiotemporal distribution of snowmelt and rainfall and their impact on river discharge. Journal of Geophysical Research: Earth Surface 115(F03019), 1-25.

Boral, S., Sen, I.S., 2020. Tracing 'Third Pole' ice meltwater contribution to the Himalayan rivers using oxygen and hydrogen isotopes. Geochemical Perspectives Letters 13, 48-53.

Burkhart, P.A., Alley, R.B., Thompson, L.G., Balog, J.D., Baldauf, P., Baker, G.S., 2017. Savor the cryosphere. GSA Today 27, 4-10.

Craig, H., 1961. Isotopic variations in meteoric waters. Science 133(3465), 1702-1703.

Dansgaard, W., 1964. Stable isotopes in precipitation. tellus 16(4), 436-468.

Deshpande, R.D., Bhattacharya, S.K., Jani, R.A., Gupta, S.K., 2003. Distribution of oxygen and hydrogen isotopes in shallow groundwaters from Southern India: influence of a dual monsoon system. Journal of Hydrology 271(1-4), 226-239.

Diamond, R.E., 2022. Stable Isotope Hydrology. The Groundwater Project, Guelph, Ontario, Canada.

Ganguly, A., Oza, H., Padhya, V., Pandey, A., Chakra, S., Deshpande, R.D., 2023. Extreme local recycling of moisture via wetlands and forests in North-East Indian subcontinent: A Mini-Amazon. Scientific Reports 13(1), 521.

Gao, J., Yao, T., Masson-Delmotte, V., Steen-Larsen, H.C., Wang, W., 2019. Collapsing glaciers threaten Asia’s water supplies. Nature 565(7737), 19-21.

Gao, M., Chen, X., Wang, J., Soulsby, C., Cheng, Q., 2021. Climate and landscape controls on spatio-temporal patterns of stream water stable isotopes in a large glacierized mountain basin on the Tibetan Plateau. Science of the Total Environment 771, 144799.

Gat, J., 2010. Isotope hydrology: a study of the water cycle. World Scientific.

Gat, J.R., Gonfiantini, R., 1981. Stable isotope hydrology. Deuterium and oxygen-18 in the water cycle. A monograph prepared under the aegis of the IAEA/UNESCO working group on nuclear techniques in hydrology of the international hydrological programme.

Gat, J.R., 1996. Oxygen and hydrogen isotopes in the hydrologic cycle. Annual Review of Earth and Planetary Sciences 24(1), 225-262.

Gaur, S., Singh, B., Bandyopadhyay, A., Stisen, S., Singh, R., 2022. Spatial pattern-based performance evaluation and uncertainty analysis of a distributed hydrological model. Hydrological Processes 36(5), 14586.

Goswami, D.C., 1985. Brahmaputra River, Assam, India: Physiography, basin denudation, and channel aggradation. Water Resources Research 21(7), 959-978.

Hren, M.T., Bookhagen, B., Blisniuk, P.M., Booth, A.L., Chamberlain, C.P., 2009. $\delta^{18}O$ and δD of streamwaters across the Himalaya and Tibetan Plateau: Implications for moisture sources and paleoelevation reconstructions. Earth and Planetary Science Letters 288(1-2), 20-32.

Jeelani, G., Deshpande, R.D., Galkowski, M., Rozanski, K., 2018. Isotopic composition of daily precipitation along the southern foothills of the Himalayas: impact of marine and continental sources of atmospheric moisture. Atmospheric Chemistry and Physics 18(12), 8789-8805.

Jeelani, G.H., Shah, R.A., Jacob, N., Deshpande, R.D., 2017. Estimation of snow and glacier melt contribution to Liddar stream in a mountainous catchment, western Himalaya: an isotopic approach. Isotopes in Environmental and Health Studies 53(1), 18-35.

Klaus, J., McDonnell, J.J., 2013. Hydrograph separation using stable isotopes: Review and evaluation. Journal of hydrology 505, 47-64.

Krishan, G., Lapworth, D.J., MacDonald, A.M. Rao, M.S., 2023. Groundwater recharge sources and processes in northwest India: Evidence from high frequency water isotope observations. Journal of Hydrology: Regional Studies 50, 101570.

Kumar, U.S., Kumar, B., Rai, S.P., Sharma, S., 2010. Stable isotope ratios in precipitation and their relationship with meteorological conditions in the Kumaon Himalayas, India. Journal of Hydrology 391(1-2), 1-8.

Kumar, V., Jain, S.K., Singh, Y., 2010. Analysis of long-term rainfall trends in India. Hydrological Sciences Journal–Journal des Sciences Hydrologiques 55(4), 484-496.

Laskar, A.H., Ramesh, R., Burman, J., Midhun, M., Yadava, M.G., Jani, R.A., Gandhi, N.,

2015. Stable isotopic characterization of Nor'westers of southern Assam, NE India. Journal of Climate Change 1(1-2), 75-87.

Lindström, G., Pers, C., Rosberg, J., Strömqvist, J., Arheimer, B., 2010. Development and testing of the HYPE (Hydrological Predictions for the Environment) water quality model for different spatial scales. Hydrology research 41(3-4), 295-319.

Mazor, E., 1990. Applied chemical and isotopic groundwater hydrology.

Mook, W.G., 2000. Environmental isotopes in the hydrological cycle: principles and applications.

Nan, Y., Tian, L., He, Z., Tian, F., Shao, L., 2021. The value of water isotope data on improving process understanding in a glacierized catchment on the Tibetan Plateau. Hydrology and Earth System Sciences 25(6), 3653-3673.

Pandey, A., Padhya, V., Chakra, S., Ganguly, A., Deshpande, R.D., 2023. Groundwater recharge in central India and its spatio-temporal variation: Insights and implications from oxygen and hydrogen isotopes. Journal of Hydrology 617, 129040.

Penna, D., Engel, M., Mao, L., Dell'Agnese, A., Bertoldi, G., Comiti, F., 2014. Tracer-based analysis of spatial and temporal variations of water sources in a glacierized catchment. Hydrology and Earth System Sciences 18(12), 5271-5288.

Piao, S., Ciais, P., Huang, Y., Shen, Z., Peng, S., Li, J., Zhou, L., Liu, H., Ma, Y., Ding, Y., Friedlingstein, P., 2010. The impacts of climate change on water resources and agriculture in China. Nature 467(7311), 43-51.

Pranavananda, S., 1939. The sources of the Brahmaputra, Indus, Sutlej, and Karnali: with notes on Manasarowar and Rakas Tal. The Geographical Journal 93(2), 126-135.

Rai, S.P., Noble, J., Singh, D., Rawat, Y.S., Kumar, B., 2021. Spatiotemporal variability in stable isotopes of the Ganga river and factors affecting their distributions. Catena 204, 105360.

Rai, S.P., Singh, D., Rai, A.K., Kumar, B., 2017. Application of environmental isotopes and hydrochemistry in the identification of source of seepage and likely connection with lake water in Lesser Himalaya, Uttarakhand, India. Journal of Earth System Science 126, 1-12.

Rautela, K.S., Kumar, D., Gandhi, B.G.R., Kumar, A., Dubey, A.K., 2023. Long-term hydrological simulation for the estimation of snowmelt contribution of Alaknanda River Basin, Uttarakhand using SWAT. AQUA—Water Infrastructure, Ecosystems and Society 72(2), 139-159.

Ren, W., Yao, T., Xie, S., 2016. Water stable isotopes in the Yarlungzangbo headwater region and its vicinity of the southwestern Tibetan Plateau. Tellus B: Chemical and Physical Meteorology 68(1), 30397.

Rozanski, K., Araguas-Araguas, L., Gonfiantini, R., 1992. Relation between long-term trends of oxygen-18 isotope composition of precipitation and climate. Science 258(5084), 981-985.

Rozanski, K., Araguás-Araguás, L., Gonfiantini, R., 1993. Isotopic patterns in modern global precipitation. Climate change in continental isotopic records 78, 1-36.

Scott, C.A., Zhang, F., Mukherji, A., Immerzeel, W., Mustafa, D., Bharati, L., 2019. Water in The Hindu kush himalaya. The Hindu Kush Himalaya assessment: Mountains, climate change, sustainability and people, 257-299.

Singh, P., Haritashya, U.K. and Kumar, N., 2008. Modelling and estimation of different components of streamflow for Gangotri Glacier basin, Himalayas. Hydrological sciences journal 53(2), 309-322.

Singh, V.., Sharma, N., Ojha, C.S.P., 2004. The Brahmaputra basin water resources, Water Science and Technology Library. Springer Netherlands.

Swain, S., Verma, M.K. and Verma, M.K., 2018. Streamflow estimation using SWAT model over Seonath river basin, Chhattisgarh, India. In Hydrologic Modeling: Select Proceedings of ICWEES-2016. Springer Singapore, 659-665.

Taia, S., Erraioui, L., Arjdal, Y., Chao, J., El Mansouri, B., Scozzari, A., 2023. The application of SWAT model and remotely sensed products to characterize the dynamic of streamflow and snow in a mountainous watershed in the High Atlas. Sensors 23(3), 1246.

Terzer, S., Wassenaar, L.I., Araguás-Araguás, L.J., Aggarwal, P.K., 2013. Global isoscapes for $\delta^{18}O$ and $\delta^{2}H$ in precipitation: improved prediction using regionalized climatic regression models. Hydrology and Earth System Sciences 17, 1–16.

Tshering, D., Dendup, T., Miller, H.A., Hill, A.F., Wilson, A.M., 2020. Seasonal source water and flow path insights from a year of sampling in the Chamkhar Chhu basin of Central Bhutan. Arctic, Antarctic, and Alpine Research 52(1), 146-160.

Vitvar, T., Aggarwal, P.K., 2012. Monitoring isotopes in rivers: Creation of the Global Network of Isotopes in Rivers (GNIR): Results of a coordinated research project 2002-2006. International Atomic Energy Agency.

Vitvar, T., Aggarwal, P.K., McDonnell, J.J., 2005. A review of isotope applications in catchment hydrology. Isotopes in the water cycle: Past, present and future of a developing science, 151-169.

Vörösmarty, C.J., McIntyre, P.B., Gessner, M.O., Dudgeon, D., Prusevich, A., Green, P., Glidden, S., Bunn, S.E., Sullivan, C.A., Liermann, C.R., Davies, P., 2010. Global threats to human water security and river biodiversity. nature 467(7315), 555-561.

Wu, H., Wu, J., Sakiev, K., Liu, J., Li, J., He, B., Liu, Y., Shen, B., 2019. Spatial and temporal variability of stable isotopes ($\delta^{18}O$ and $\delta^{2}H$) in surface waters of arid, mountainous Central Asia. Hydrological Processes 33(12), 1658-1669.

Zhou, J., Wu, J., Liu, S., Zeng, G., Qin, J., Wang, X., Zhao, Q., 2015. Hydrograph separation in the headwaters of the Shule River basin: combining water chemistry and stable isotopes. Advances in Meteorology 2015(1), 830306.